LONGITUDINAL MICROWAVE INSTABILITY STUDY AT TRANSITION CROSSING WITH ION BEAMS IN THE CERN PS

A. Lasheen*, B. Popovic, H. Damerau, A. Huschauer, CERN, Geneva, Switzerland

Abstract

The luminosity of lead ion collisions in the Large Hadron Collider (LHC) was significantly increased during the 2018 ion run by reducing the bunch spacing from 100 ns to 75 ns, allowing to increase the total number of bunches. With the new 75 ns variant, three instead of four bunches are generated each cycle in the Low Energy Ion Ring (LEIR) and the Proton Synchrotron (PS) with up to 30% larger intensity per bunch. The beam was produced with satisfactory quality but at the limit of stability in the injectors. In particular, the minimum longitudinal emittance in the PS is limited by a strong longitudinal microwave instability occurring just after transition crossing. The uncontrolled blow-up generates tails, which translates into unacceptably large satellite population following the RF manipulations prior to extraction from the PS. In this paper, instability measurements are compared to particle tracking simulations using the latest PS impedance model to identify the driving impedance sources. Moreover, means to mitigate the instability are discussed.

INTRODUCTION

The 2018 ion run in the LHC established a record in terms of integrated luminosity, reaching values close to the ones expected in the framework of the High Luminosity LHC project [1]. A main ingredient to reach this performance was the reduction of the bunch spacing in the injectors, allowing to increase the total number of bunches in the LHC.

A new scheme was put in operation in 2018 which consisted of reducing the bunch spacing from 100 ns to 75 ns in the PS by applying a batch compression at top energy. This operation involves RF systems tuned at harmonic numbers $h = 21$ (10 MHz) and $h = 28$ (13 MHz). Moreover, 3 bunches instead of 4 were generated in the LEIR and injected into $h = 24$ RF buckets in the PS. A measurement of the RF manipulation at top energy is shown in Fig. 1.

For all ion beams produced in the PS, a rebucketing to $h = 169$ (80 MHz) is performed prior to an adiabatic bunch shortening and extraction to the SPS. The bucket length before and after the rebucketing is greatly reduced due to the large harmonic ratio. Therefore, the bunch length (i.e. longitudinal emittance) should remain sufficiently small to avoid losing particles or capturing particles in neighboring buckets as illustrated in Fig. 1 (top, satellite bunches).

The total beam intensity provided by the LEIR remains almost identical with 3 or 4 extracted bunches. Hence, the single bunch intensity in the PS for the 75 ns bunch spacing scheme is about 30% larger than the nominal one. This increase of the single bunch intensity led to the observation of a beam instability at transition crossing in the PS,
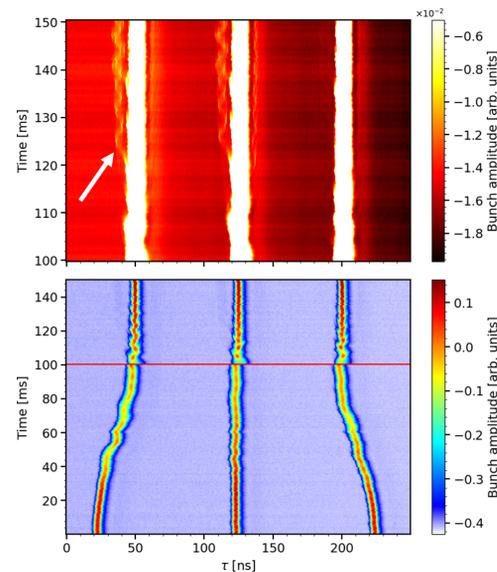
_____
* alexandre.lasheen@cern.ch

Figure 1: Evolution of bunch profiles during the batch compression ($h = 21 \rightarrow h = 28$) at top energy in the PS to bring the bunch spacing from 100 ns to 75 ns. The batch compression is followed by a rebucketing ($h = 28 \rightarrow h = 169$). The upper plot shows the generation of satellite bunches during rebucketing (from red marker on bottom plot, adjusted color scale).

manifesting as uncontrolled emittance blow-up. This turned out to be comparable to instabilities observed under similar conditions in the KEK-PS [2]. In this paper, we show measurements of the beam instability and identification of the impedance sources, followed by comparison with particle tracking simulations.

MEASUREMENTS OF THE INSTABILITY

A typical evolution of the bunch profile is shown in Fig. 2 (left). Shortly after transition crossing, a high frequency modulation appears on the bunch profile bearing the signature of a longitudinal microwave instability. After the initial fast break-up, the bunch resumes its normal synchrotron motion before arriving to top energy with a large, uncontrolled longitudinal emittance.

In the PS, six high frequency cavities tuned to 200 MHz are available for controlled longitudinal emittance blow-up (BUP) with phase modulation [3]. Enabling three of these at an amplitude of 3 kV generated sufficient controlled emittance blow-up to stabilize the beam as seen in Fig. 2 (middle). A good compromise between beam stability and generation of satellite bunches during rebucketing was found in operation. Nonetheless, the margin in terms of longitudinal emittance and beam intensity remained small.
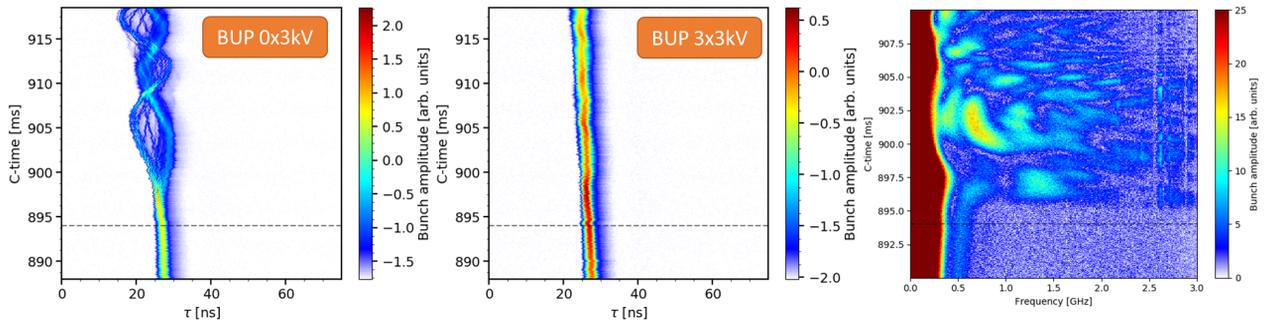
Figure 2: Evolution of the bunch profile at transition crossing. The beam is unstable at transition crossing (left) and stabilized with controlled emittance blow-up before transition (middle, with 3 cavities pulsing at 3 kV). The bunch spectrum corresponding to the unstable case is displayed on the right. The dashed line represents the moment of the RF phase jump for transition crossing.

The evolution of the bunch spectrum during the instability is shown in Fig. 2 (right). The spectrum can be decomposed in two parts: the stationary spectrum at low frequency S_0 and the (unstable) spectrum S_1 from the perturbation at high frequency. When the synchrotron motion is frozen like at transition crossing, longitudinal microwave instability can be driven by narrow-band impedance sources with $f_r \tau_l \gg 1$ where f_r is the resonance frequency of the impedance source and τ_l the bunch length [4, 5]. In that context and assuming a Gaussian stationary component, the unstable beam spectrum is

$$S_1 \sim n S_0 (n - n_r) \sim n e^{-\frac{\sigma_{\mathrm{rms}}^2 (n-n_r)^2}{2}}, \qquad (1)$$

where $n = f/f_{\mathrm{rev}}$ is the revolution frequency (f_{rev}) index, $n_r = f_r/f_{\mathrm{rev}}$ is the impedance resonant frequency index exciting the instability and σ_{rms} is the rms bunch length.

According to Eq. (1), the unstable spectrum is centered around the resonant frequency of the driving impedance and can therefore be used as a estimator of f_r. However, the width of S_1 is of the order of the stationary one. Bunches are very short (≈ 3 ns) at transition crossing implying that the increased width of S_1 will cause a large uncertainty to the exact value of f_r. In Fig. 2 (right), the first modulation right after transition crossing suggests an impedance source at $f_r = 1.3 \pm 0.2$ GHz. Other candidates were also measured at $f_r = 1.6 \pm 0.3$ GHz and $f_r = 2.4 \pm 0.4$ GHz.

IDENTIFICATION OF THE IMPEDANCE SOURCE

A thorough survey of the devices that could contribute to the longitudinal beam-coupling impedance was conducted over the past years to study beam instabilities [6, 7]. Two possible contributors corresponding to the measured f_r with beam are the unshielded pumping manifolds and the sector valves as presented in Fig. 3.

A hundred pumping manifolds are installed in the PS downstream of each main magnet unit. A pick-up for the beam trajectory measurement system [8] is inserted in most of them, acting also as a partial impedance shield. Nonetheless, about one third is left empty causing a large longitudinal impedance with multiple resonant frequencies at

$f_r \approx 1.3$ GHz, compatible with the measured modulation on Fig. 2. These pumping manifolds were already suspected decades ago to be responsible for longitudinal microwave instabilities in the PS [9], and damping resistors were inserted to reduce the quality factor of the resonance, with limited effect on the measured instability.
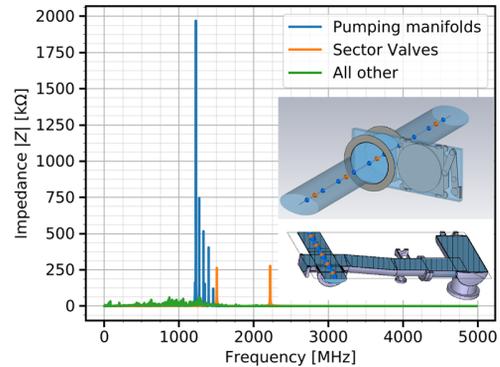

Figure 3: The PS impedance model at high frequency. The PS sector valves (top) and unshielded pumping manifolds (bottom) modeled with the CST software [10].

Additionally, ten sector valves are installed in the PS and also contribute to the longitudinal impedance at resonant frequencies at $f_r = 1.50$ GHz and $f_r = 2.28$ GHz which are also compatible with the ones measured with beam [11].

MODELING TRANSITION CROSSING

Simulations were performed using the BLonD tracking code [12] to assess whether the suspected impedance sources can indeed be responsible for the observed instability. Simulations are started 200 ms before transition crossing to begin with stationary conditions during the ramp.

Several challenges were faced to introduce all features at transition crossing. The first step was to include transition crossing with the γ_t jump scheme [13]. The evolution of the beam Lorentz factor γ and the transition γ_t is plotted in Fig. 4. The linear γ_t was calculated every millisecond with the MAD-X code [14], using the programmed strengths for the fast quadrupole magnets. Note that transition with the

12th Int. Particle Acc. Conf.   IPAC2021, Campinas, SP, Brazil   JACoW Publishing

ISBN: 978-3-95450-214-1   ISSN: 2673-5490   doi:10.18429/JACoW-IPAC2021-WEPAB243
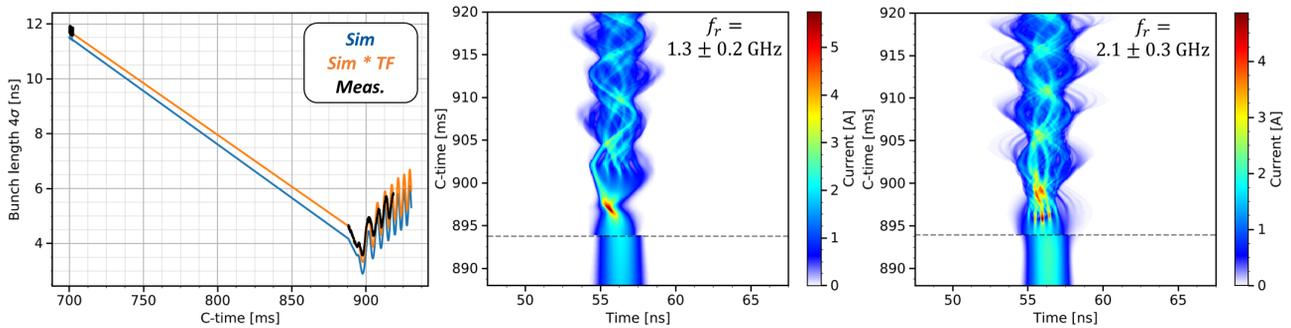
Figure 5: Simulated transition crossing. On the left, the simulated bunch length (colored) is compared with measurements (black) for a stable situation with large longitudinal emittance. The measured bunch lengthening due to attenuation of the cables is taken into account in simulations (blue vs. orange). The simulated profiles for unstable beam with low longitudinal emittance are displayed including the γ_t jump (middle), and without (right). The main high frequency modulation is specified for each case.

ion beam is crossed at higher magnetic fields compared to the proton beam (different γ for constant γ_t), for which the scheme was originally designed. Therefore, the amplitude of the γ_t jump is small and saturation of the main dipole magnets had to be taken into account for better comparison with measurements.
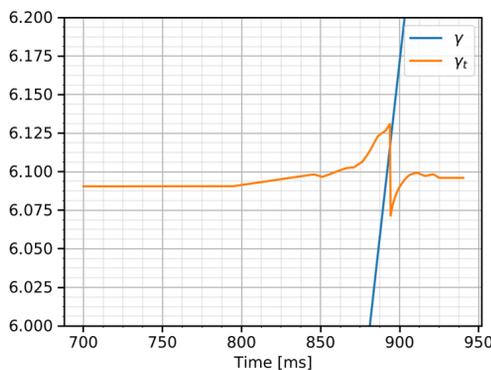

Figure 4: The beam γ and transition γ_t at transition crossing with the ion beam.

The longitudinal space charge, which is modeled as a pure reactive impedance, also gives a relevant impedance contribution. Space charge forces are defocusing below transition and focusing above. This contributes to the mismatch manifesting as bunch length oscillations after transition which can be observed both in simulated and measured bunch lengths in Fig. 5 (left). To reach good agreement, the longitudinal space charge was reduced by 30% in the model. It indicates that either the space charge model should be refined, or that inductive impedance is missing from the model.

The result of the simulation is displayed in Fig. 5 (middle). A high frequency modulation can be seen after transition with a frequency of $f_r = 1.3$ GHz corresponding to the effect of the unshielded pumping manifolds. Although the instability is well reproduced under the same conditions in terms of bunch intensity and emittance, the exact pattern does not match exactly the measured one. A strong longitudinal focusing is seen before the high frequency modulation,

occurring with a delay of 5 ms with respect to measurements. Further tests were performed by removing the γ_t jump to evaluate its contribution. The result is shown in Fig. 5 (right) and indicates that, despite its small amplitude, the γ_t jump has an important influence on the beam. Indeed, the strong focusing disappeared, and the modulation frequency is now at $f_r = 2.1$ GHz and increased in amplitude. The influence of the γ_t jump was already noticed in [2] and should have a stabilizing effect.

Despite the complexity of the simulation, the instability is reproduced with a slightly different pattern with respect to measurements. Further refinement is foreseen to obtain a better agreement, more specifically on modeling of space charge and the completion of the impedance model, the γ_t jump with non-linear momentum compaction factor and implementation of beam control loops.

CONCLUSIONS

A longitudinal microwave instability was measured at transition crossing with the ion beam. Although the limitation was solved in operation with controlled emittance blow-up, detailed studies were conducted to find the impedance source responsible for the instability. Preliminary investigations hint at the unshielded pumping manifolds and the sector valves as driving impedance sources. A qualitative agreement is obtained in simulations where the amplitude of the γ_t jump was shown to be important. Possible mitigations of the instability would be to increase the amplitude of the γ_t jump or impedance reduction by shielding primarily the empty pumping manifolds, with additional inserts. Finally, this study can finally be used a benchmark to evaluate the threshold of microwave instability for the proton beam.

ACKNOWLEDGMENTS

MC5: Beam Dynamics and EM Fields

D06 Coherent and Incoherent Instabilities - Measurements and Countermeasures

REFERENCES

[1] J. Jowett *et al.*, "The 2018 Heavy-Ion Run of the LHC", in *Proc. 10th International Particle Accelerator Conference (IPAC'19)*, Melbourne, Australia, May 2019, pp. 2258–2261. `doi:10.18429/JACoW-IPAC2019-WEYYPLM2`

[2] K. Takayama, D. Arakawa, J. Kishiro, K. Koba, and M. Yoshii, "Microwave Instability at Transition Crossing: Experiments and a Proton-Klystron Model", *Phys. Rev. Lett.*, vol. 78, pp. 871–874, 1997. `doi:10.1103/PhysRevLett.78.871`

[3] H. Damerau, M. Morvillo, E. Shaposhnikova, J. Tückmantel, and J. L. Vallet, "Controlled Longitudinal Emittance Blow-Up in the CERN PS", CERN, Geneva, Switzerland, Tech. Rep. CERN-AB-2007-052, 2007.

[4] T. Bohl, T. P. R. Linnecar, and E. Shaposhnikova, "Measuring the Resonance Structure of Accelerator Impedance with Single Bunches", *Phys. Rev. Lett.*, vol. 78, pp. 3109–3112, 1997.
`doi:10.1103/PhysRevLett.78.3109`

[5] A. Lasheen, T. Argyropoulos, T. Bohl, J. F. Esteban Müller, H. Timko, and E. Shaposhnikova, "Beam measurement of the high frequency impedance sources with long bunches in the CERN Super Proton Synchrotron", *Phys. Rev. Accel. Beams*, vol. 21, p. 034 401, 2018.
`doi:10.1103/PhysRevAccelBeams.21.034401`

[6] M. Migliorati, S. Persichelli, H. Damerau, S. Gilardoni, S. Hancock, and L. Palumbo, "Beam-wall interaction in the CERN Proton Synchrotron for the LHC upgrade", *Phys. Rev. ST Accel. Beams*, vol. 16, p. 031 001, 2013.
`doi:10.1103/PhysRevSTAB.16.031001`

[7] PS Longitudinal Impedance Model, `https://zenodo.org/record/4722835`.

[8] J. J. Belleman, "A new trajectory measurement system for the CERN proton synchrotron", CERN, Geneva, Switzerland, Tech. Rep. CERN-AB-2005-059, 2005.

[9] D. Boussard, "Observation of microwave longitudinal instabilities in the CPS", CERN, Geneva, Switzerland, Tech. Rep. CERN-LabII-RF-INT-75-2, 1975.

[10] CST Studio Suite, Electromagnetic Field Simulation Software, `https://www.cst.com`.

[11] B. Popovic and C. Vollinger, "Beam Impedance Evaluation for CERN PS Gate Valves by Simulation and Benchmark Measurement", in *Proc. 9th International Particle Accelerator Conference (IPAC'18)*, Vancouver, Canada, Apr. 2018, pp. 3080–3082.
`doi:10.18429/JACoW-IPAC2018-THPAF051`

[12] CERN Beam Longitudinal Dynamics code BLonD, `https://blond.web.cern.ch/`.

[13] A. Sørensen, "Crossing The Phase Transition In Strong Focusing Proton synchrotrons", *Part. Accel.*, vol. 6, pp. 141–165, 1975.

[14] MAD - Methodical Accelerator Design, `http://madx.web.cern.ch/madx/`.